CrystEngComm

PAPER

View Article Online
View Journal | View Issue



Cite this: *CrystEngComm*, 2019, **21**, 1635

# Two novel multichromic coordination polymers based on a new flexible viologen ligand exhibiting photocontrolled luminescence properties and sensitive detection for ammonia†

Hai Yu Wang, Shuang Liu, Chen Fu and Hong Zhang *

A new flexible bipyridinium ligand, 1,1′-bis-((3-carboxylatobenzyl)-4,4′-bipyridinium) dichloride ($H_2$bcbpy·2Cl), was synthesized and successfully introduced into two novel cadmium-based coordination polymers (CPs) by analogous solvothermal reactions. Because of the presence of electron-deficient bipyridinium moieties, compounds **1** and **2** can both easily undergo photo- and thermal-induced electron transfer and exhibit eye-detectable photochromic and thermochromic behaviors. Moreover, their luminescence properties can be switched by UV-vis light irradiation or by heating to 90 °C. Interestingly, **1** and **2** have a sensitive response for ammonia. The yellow compounds **1** and **2** turn blue and green, respectively, when exposed to ammonia vapor. For most CPs-based bipyridinium derivatives, their crystal structures are usually damaged when exposed to ammonia vapor. Surprisingly, compound **2** displays a fast discolored–decolored response to ammonia within dozens of seconds and maintains an unchanged crystal structure.

Received 14th November 2018,
Accepted 27th January 2019

DOI: 10.1039/c8ce01948g

rsc.li/crystengcomm



## Introduction

Coordination polymers (CPs) as breakthrough materials with various structures can be designed to cater for the increasing demands in the fields of magnetic materials; gas storage, its separation and catalysis; and so on.[1–4] In recent years, CPs with colour-changing properties, one of the most common and useful species, have attracted tremendous attention owing to their increasing demands in the fields of energy storage,[5] sensors,[6] drug delivery,[7] and proton conductivity.[8] Many families of organic and inorganic multichromic materials have been explored, where organic species are the major development objects, as they can be easily modified by the functional groups.[9] The ability to chemically modify the organic ligands specifically for their desirable optical properties is an important strategy in designing materials with new and functional applications.[10] For example, piperazine-, diarylethene-, and naphthalenediimide-based CPs have been fabricated as multichromic materials applied in photochemistry and thermochemistry.[11–13] Viologen/bipyridinium derivatives (1,1′-disubstituted 4,4′-bipyridinium) have a long history of research and development as herbicides used in a wide variety of pharmaceuticals and medicine. Recently, viologen derivatives have been researched deeply in the field of multichromic materials, such as photochromic, thermochromic, electrochromic and sensing materials, due to their excellent electron-accepting abilities and Lewis acidic sites.[14–16] The electron-deficient viologen cation ($V^{2+}$) is capable of forming the viologen cationic radical ($V^{+}$) through one-electron transfer from the appropriate electron donors and usually can be accompanied with recognizable colour changes.[17] Thus, one of the interesting properties of viologens is chromic progress, which arises from electron transfer (ET) progress from the electron donors (D) to the electron acceptor (A = viologens).[18] Therefore, viologen derivatives as outstanding candidates have been used in multichromic material designs.[9e] To construct chromic viologen-based CPs with the electron transfer (ET) progress, some key factors should be considered, such as the packing type, the distance and orientation between the D and the A, hydrogen bonds and so on.[19,20] Although numerous chromic families based on ET chemical processes have been reported to date, for multichromic CPs, there are relatively few that have been reported.[9e,21] If a single material displays both photochromic behavior and thermochromic behavior, more extensive functions and applications will be expected.[22] Because of the excellent characteristic of viologen/bipyridinium derivatives, we envisaged that it should be

*Institute of Polyoxometalate Chemistry, Department of Chemistry, Northeast Normal University, Changchun, Jilin 130024, PR China.*
*E-mail: hope20130122@163.com*

† Electronic supplementary information (ESI) available: Graphics (Fig. S1–S19) and tables (Tables S1 and S2). CCDC 1586364 and 1810868. For ESI and crystallographic data in CIF or other electronic format see DOI: 10.1039/c8ce01948g

suitable for selecting viologens as the organic ligands and to introduce the viologen moiety into CPs to construct new-type multichromic materials.

Herein, a new carboxylate-derived viologen ligand, 1,1′-bis-((3-carboxylatobenzyl)-4,4′-bipyridinium)-dichloride (**$H_2$bcbpy·2Cl**), was synthesized and successfully used to construct two novel viologen-based CPs, [Cd(bcbpy)$Br_2(H_2O)_2$] (**1**) and [Cd(bcbpy)$(SCN)_2$] (**2**), which have rare multichromic properties. Compounds **1** and **2** display both photochromism and thermochromism. Besides, compounds **1** and **2** also have photo- and thermocontrolled luminescence properties. Notably, owing to the Lewis acidity of the bcbpy ligand, **1** and **2** exhibit good ammonia detection abilities; when exposed to ammonia vapour, they all showed significant color changes. However, because of the different coordination environments of the metal centers and the packing structures of the two compounds, compounds **1** and **2** exhibit different phenomena and results when exposed to ammonia vapor. In our work, UV-vis-NIR spectrophotometer, electron spin resonance (ESR), and density functional theory (DFT) calculations were performed to provide valuable insight into the explorations of a mechanism for chromism and ammonia detection. Our work is conducive to guiding the design and synthesis of new multifunctional viologen-based CPs.

# Experimental

### Materials and methods

All materials were purchased commercially and used without further purification. **$H_2$bcbpy·2Cl** was synthesized as shown in Scheme 1. Elemental analyses (C, H and N) were performed using a PerkinElmer 2400 CHN elemental analyzer. The infrared spectra were measured in the range of 400–4000 $cm^{-1}$ using a Mattson Alpha-Centauri spectrometer with KBr pellets. The powder X-ray diffraction (PXRD) patterns were recorded using a RigakuDmax 2000 X-ray diffractometer with graphite monochromatized Cu Kα radiation ($\lambda$ = 0.15418 nm) and 2$\theta$ ranging from 5° to 50° at room temperature. Thermogravimetric analyses (TGA) of crystalline samples were performed using a PerkinElmer thermal analyzer under nitrogen at a heating rate of 10 °C $min^{-1}$ in the range of 30–800 °C. The UV-vis absorption studies were measured using a Cary 700 UV-vis-NIR spectrophotometer. Electron spin resonance (ESR) studies were carried out at X-band frequency (9.45 GHz) on a Bruker EMX spectrometer, and fluorescence spectra were obtained using a FLSP920 fluorescence spectrometer.

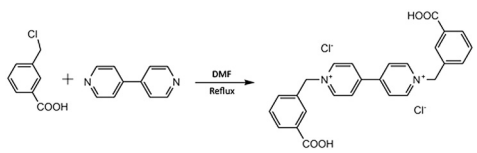


**Scheme 1** Synthesis of the **$H_2$bcbpy·2Cl** ligand.

**Synthesis of $H_2$bcbpy·2Cl.** 1,1′-Bis-((3-carboxylatobenzyl)-4,4′-bipyridinium) dichloride ligand (**$H_2$bcbpy·2Cl**) was synthesized based on the nucleophilic substitution reaction of 4,4′-bipyridine and 3-(chloromethyl)-benzoic acid (Scheme 1). 4,4′-Bipyridine (2.00 g, 12.8 mmol) and 3-(chloromethyl)-benzoic acid (6.56 g, 38.4 mmol) were dissolved in 13 mL of DMF, and the mixture was stirred at 120 °C for 8 h. The resultant yellow precipitate was isolated by filtration and washed with hot DMF solution three times, producing 1,1′-bis-((3-carboxylatobenzyl)-4,4′-bipyridinium) dichloride with 4,4′-bipyridine. The reaction product was then purified by recrystallization with acetone and deionized water (1 : 1, V/V) to obtain a pale yellow solid **$H_2$bcbpy·2Cl**. Yield: 89%. **$^1$H-NMR** (600 MHz, $D_2O$): $\delta$ = 9.18 (d, $J$ = 7.2 Hz, 4H), 8.55 (d, $J$ = 6.6 Hz, 4H), 8.09 (d, $J$ = 7.8 Hz, 4H), 7.75 (d, $J$ = 7.8 Hz, 2H), 7.62 (t, $J$ = 7.2 Hz, 2H), 6.00 (s, 2H). **$^{13}$C-NMR** (151 MHz, $D_2O$): $\delta$ = 169.5, 150.4, 145.6, 134.1, 132.7, 131.1, 131.1, 130.2, 130.0, 127.3, 64.2.

**Synthesis of [Cd(bcbpy)$Br_2(H_2O)_2$] (1).** The reaction mixture containing **$H_2$bcbpy·2Cl** (49.7 mg, 0.1 mmol), $Cd(NO_3)_2 \cdot 4H_2O$ (0.0308 g, 0.1 mmol), KBr (23.8 mg, 0.2 mmol), DMF (2 mL), EtOH (1 mL), and distilled water (3 mL) was sealed in a 25 mL Teflon reactor autoclave and heated to 75 °C for 2 days. After cooling to room temperature at a rate of 5 °C $h^{-1}$, the obtained yellow single crystals of **1** were collected and washed with deionized water and then dried in air. Yield: 83% based on **$H_2$bcbpy·2Cl**. Anal. calcd. (%) for $C_{26}H_{24}N_2O_6Br_2Cd$: C, 42.62; H, 3.28; N, 3.82%. Found: C, 41.90; H, 3.46; N, 3.73%.

**Synthesis of [Cd(bcbpy)$(SCN)_2$] (2).** The reaction mixture containing **$H_2$bcbpy·2Cl** (49.7 mg, 0.1 mmol), $Cd(NO_3)_2 \cdot 4H_2O$ (0.0308 g, 0.1 mmol), KSCN (19.4 mg, 0.2 mmol), DMF (2 mL), EtOH (1 mL) and distilled water (3 mL) was sealed in a 25 mL Teflon reactor autoclave and heated to 75 °C for 2 days. After cooling to room temperature at a rate of 5 °C $h^{-1}$, the obtained light yellow single crystals of **2** were collected and washed with deionized water and then dried in air. Yield: 76% based on **$H_2$bcbpy·2Cl**. Anal. calcd. (%) for $C_{28}H_{20}N_4O_4S_2Cd$: C, 51.50; H, 3.06; N, 8.58%. Found: C, 51.11; H, 3.19; N, 8.51%.

### X-ray diffraction analysis

Crystal data for **1** and **2** were collected using an Oxford Diffraction Gemini R Ultra diffractometer with graphite-monochromated Mo-Kα radiation ($\lambda$ = 0.71073 Å) at 296 K. Absorption correction was applied using the multiscan technique. The structures were solved and refined by full-matrix least-squares on $F^2$ using the program packages of Olex2 and SHELXTL2014.[23,24] Thermal parameters of all non-hydrogen atoms of the compounds were refined anisotropically, and hydrogen atoms on organic ligands were fixed at calculated positions. All of the crystal data and the structure refinements are summarized in Table S1.† The main bond lengths and angles for **1** and **2** are shown in Table S2.† Crystallographic data were deposited with the Cambridge

 

Crystallographic Data Center (CCDC) as supplementary publication numbers CCDC 1586364 (compound **1**) and 1810868 (compound **2**), respectively.

## Theoretical study

The molecule frontier orbitals were analyzed by density functional theory (DFT) to further demonstrate the mechanism of photochromism, based on the X-ray crystallographic data of **1** and **2**. The DMol$^3$ Module[25] in the Materials Studio (MS) 7.0 software package[26] was used with a ($10^{-6}$ eV per atom) tolerance for SCF convergence. The DFT exchange–correlation potential was described by the Perdew–Burke–Ernzerhof (PBE) functional within the generalized gradient approximation (GGA).[27] The Grimme scheme was applied for dispersion corrections, and the double numerical plus polarization (DNP) basis set was used for a better orbital cutoff quality.[28]

To investigate the chromic mechanism of ammonia detection in CPs based on viologens, the crystal structures of **1**, **2** and $NH_3$ were optimized by DFT calculations using the DMol$^3$ Module. The GGA-PBE exchange–correlation functional and the Grimme dispersion-correction scheme were applied to optimize. A fine optimization convergence level was selected, with an energy tolerance of $10^{-5}$ eV per atom and a maximum displacement of 0.001 Å.

## Results and discussion

### Crystal structure of $[Cd(bcbpy)Br_2]\cdot(H_2O)_2$ (1)

Single-crystal X-ray diffraction analysis indicates that compound **1** crystallizes in the monoclinic space with group $P2_1/c$; the asymmetric unit of compound **1** consists of one Cd(II) ion, one bcbpy ligand, two Br anions and two dissociative water molecules. As shown in Fig. 1a, Cd(II) is five-coordinated by three O atoms belonging to two different bcbpy ligands and two $Br^-$ anions from KBr, forming a monodentate coordination with O1 and a bidentate coordination with O3 and O4. As shown in Table S2,† the bond lengths of Cd1–O1 (2.216 Å), Cd1–O3 (2.308 Å), Cd1–O4 (2.416 Å), Cd1–Br1 (2.6052 Å) and Cd1–Br2 (2.5805 Å) are close to the values observed in the Cd(II) CPs reported.[16] The main bond angles are shown in Table S2.† Each Cd(II) cation is bridged with each other through the carboxylate groups from bcbpy as secondary linkers leading to a helical 1-D structure (Fig. 1c). One structural characteristic of **1** is that it has a close distance between O4 of the carboxylate groups and N2 of the viologen moiety of the bcbpy ligand ($d_{O-\pi}$ = 3.449 Å, Fig. S1a†), which is supposed to play a very important role in their electron separation and transfer upon applying external light stimuli. As displayed in Fig. S3a,† a face-to-face π–π stacking interaction forming between the pyridinium ring and a contiguous phenylene ring, with a distance of 3.402 Å, a weak π–π stacking interaction between the phenylene rings, with a distance of 4.193 Å, and O–H···O hydrogen bonds (1.866 Å and 2.175 Å, Fig. 1a) were observed, which can stabilize crystal structure well.

### Crystal structure of $[Cd(bcbpy)(SCN)_2]$ (2)

Single-crystal X-ray diffraction analysis indicates that compound **2** crystallizes in the monoclinic space with group $C2/c$; the asymmetric unit of compound **2** consists of one Cd(II) ion, one bcbpy ligand, and two $SCN^-$ anions. As shown in Fig. 1b, Cd(II) is coordinated by four O atoms belonging to two different bcbpy ligands, forming a bidentate coordination, and two N atoms from $SCN^-$. As shown in Table S2,† the bond lengths of Cd1–O1 (2.411 Å), Cd1–O1#2 (2.411 Å), Cd1–O2 (2.313 Å), Cd1–O2#2 (2.313 Å), Cd1–N1 (2.219 Å) and Cd1–N1#2 (2.219 Å), are close to the values observed in the Cd(II) CPs reported.[16] The main bond angles are displayed in Table S2.† Each Cd(II) cation is bridged with each other through the carboxylate groups as secondary linkers, leading to an infinite 1-D chain structure (Fig. 1d). Compared with **1**, as displayed in Fig. S3b,† there is a weak π–π stacking interaction between the phenylene rings, with a distance of 3.853 Å, and the distance between O2 of the carboxylate groups and N2 of the viologen moiety of the bcbpy ligand is 3.982 Å, which is the main reason to create light response rate differences between the two complexes.[29]

## Photo- and thermochromic properties

As found from many viologen-based CPs, compounds **1** and **2** have photochromic behaviors. As shown in Fig. 2a,

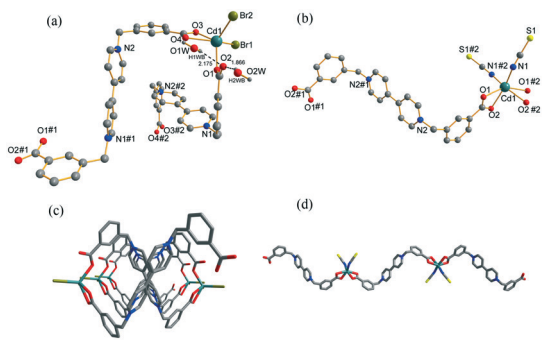


Fig. 1 (a) Coordination environment around the Cd(II) ion in **1**; (b) coordination environment around the Cd(II) ion in **2**; (c) 1D structure of **1**; (d) 1D structure of **2**. Symmetry codes: for 1: #1: *x*, 0.5 − *y*, −0.5 + *z* #2: *x*, 0.5 − *y*, 0.5 + *z*; for 2: #1: −*x*, 1 − *y*, 1 − *z* #2: 1 − *x*, *y*, 1.5 − *z*.

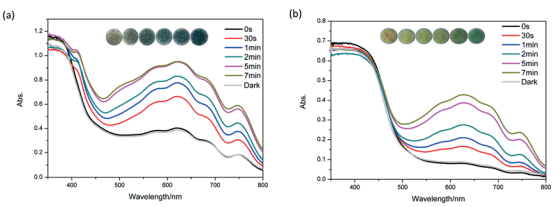


Fig. 2 (a) UV-vis spectrum and photographs of compound **1** before and after irradiation with a 300 W Xe lamp; (b) UV-vis spectrum and photographs of compound **2** before and after irradiation with a 300 W Xe lamp.

compound **1** is quite sensitive to light, since it instantaneously turns from yellow to deep blue upon exposure to solar light, or UV-vis light (Xe lamp, 300 W). When illuminated with a Xe lamp, insulated glass was used to remove the influence of heat and tends to be saturated after illumination for 5 min. Compound **2** turns green after being irradiated within 30s with UV-vis light (Xe lamp, 300 W) and tends to be saturated after illumination for 7 min (Fig. 2b). The photochromic samples can be decolored in the dark. The UV-vis diffuse reflectance spectra of compounds **1** and **2** before and after irradiation are shown in Fig. 2. Because **1** is sensitive to solar light, the original sample of **1** shows two broad absorption bands at 620 nm and 751 nm in the visible region before irradiation. After irradiation, a new narrow absorption band shows at 410 nm, which correspond to the n–π* and π–π* transitions of the bcbpy ligands (Fig. S1†), and all the absorption bands become intense with increasing irradiation time.[30] These characteristic spectral bands are similar to those observed for bipyridinium radicals, suggesting that the color change of **1** and **2** may arise from the photoinduced generation of radicals in the bcbpy ligands.[22,31,32] Nevertheless, compared with **1**, compound **2** only has adsorptions at 627 nm and 745 nm after irradiation. As shown Fig. 2, **1** has a faster photoresponse than **2**. By analyzing and comparing the interactions around the pyridinium ring (Fig. S2†), this phenomenon was determined to be mainly caused by the following three reasons: firstly, the distance between the carboxylate O atom and the N atom in **1** ($d$ = 3.449 Å) is shorter than that in **2** ($d$ = 3.982 Å), and the distance between the $Br^-$ atom and the N atom of the bcbpy ligand is 3.876 Å, which may be another pathway to satisfy the electron transfer criterion between the donor and viologen acceptor units (Fig. S1†); secondly, comparing the structures of **1** and **2**, **1** has a helical 1-D structure (Fig. S2†), forming a strong π–π stacking interaction between the pyridinium ring and a contiguous phenylene ring, promoting the ET progress (Fig. S3a†); in the end, the interactions of the O–H···O hydrogen bonds between the carboxylate group and the dissociative water molecule (O1W–H1WB···O2 and O2W–H2WB···O2) in **1** may also improve the ET (Fig. 1a). To further demonstrate the ET progress, as well as the photochromism, between the donors and viologen acceptor units, density functional theory (DFT) calculations were used to analyze the molecular frontier orbitals. Orbital analysis shows that the highest occupied molecular orbital (HOMO) arises almost solely from the p orbitals of the carboxylate oxygen atoms of the bcbpy ligand, and the lowest unoccupied molecular orbital (LUMO) is dominated by the p–p* orbitals of the viologen moiety (Fig. S4†). Therefore, it is reasonable to assume that the electron transfer occurs from carboxylate oxygen to bipyridinium, generating viologen radicals. Because of the shorter distance $d_{O-N}$ in **1**, **1** has a faster photo response than **2**.[32] Interestingly, after annealing at 90 °C for 5 minutes in air or under vacuum, the yellow complexes **1** and **2** turn green, and the absorption bands at 621 nm and 748 nm for **1** and at 630 nm and 746 nm for **2** emerged in the UV-vis spectra after thermocoloration (Fig. S5†). The thermochromic sample can be decolored in the dark and can again change to green at 90 °C, which indicates that the thermochromism is reversible.

The powder XRD profiles and infrared (IR) spectra show no appreciable variations after photo- and thermochromism (Fig. S6–S8†), suggesting that the molecular structures were maintained without bond cleavage or formation, which indicates that the origins of photochromic and thermochromic properties for the compounds **1** and **2** are not photoinduced isomerization or photolysis. As speculated, such behaviors should result from the viologen free radical generation.[14,15,22] Electron paramagnetic resonance (EPR) spectroscopies were performed to confirm the involvement of radicals in the chromic process. The EPR studies before and after irradiation and ammonia absorption have been recorded. As shown in Fig. 3, the colored states of **1** and **2** present strong EPR signals with $g$ = 1.9832 and $g$ = 1.9833, respectively, which is similar to those found in bipyridinium and viologen complexes and confirm the existence of viologen free radical generation.[16,17]

## Luminescence properties

Considering the luminescence performance of the **$H_2$bcbpy·2Cl** ligand (Fig. S9†), the $d^{10}$ Cd(II) metal ion center, as well as the photo- and thermochromic behaviors of the two CPs, photo- and thermocontrolled luminescence properties are mentioned in our study.[33] Compounds **1** and **2** all exhibit evident photocontrolled fluorescence quenching phenomena. As shown in Fig. 4a, the fluorescent spectrum of **1** explains that there is a strong emission peak at 545 nm when excited at 469 nm. Meanwhile, the fluorescence spectrum of **2** shows a strong emission peak at 551 nm, which probably originates from different coordination modes, packing structures between the two complexes (Fig. 4b). Moreover, the emission peak is fleetly and gradually reduced upon irradiation with a xenon lamp (300 W) and is almost totally quenched when **1** changes to blue after irradiation for 5 min, and **2** changes to green after irradiating for 7 min. The results illustrate that photochromism and photocontrolled luminescence can take place simultaneously, originating from photoinduced ET between the electron donor and the electron acceptor (viologens). Therefore, the emission intensity is influenced by the ET progress, which results in quenching luminescence. Besides, π–π interactions between

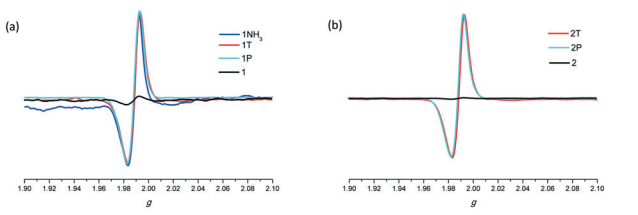


Fig. 3 The EPR spectra of **1** (a) and **2** (b); before irradiation (black), after irradiation (cyan), after heated (red) and after ammonia absorption (blue).

 

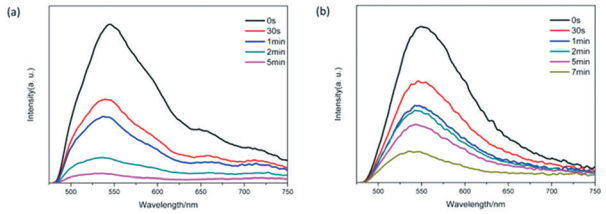


Fig. 4 The luminescence emission spectral changes ($\lambda_{ex}$ = 469 nm) of **1** (a) and **2** (b) after irradiation with a 300 W Xe lamp at different times.

the aromatic rings of two neighbouring bcbpy ligands may accelerate the ET progress and expedite the fluorescent quenching rate (Fig. S3†). The luminescence intensity recovered to its initial state when the colored crystals of **1** and **2** turn into the original yellow samples again. The luminescence property of the two compounds is reversible. Simultaneously, the thermocontrolled luminescence property was researched in our study. The thermocontrolled luminescence emission spectrum of **$H_2$bcbpy·2Cl** is displayed in Fig. S10.† Based on the excellent sensitivity to the heat stimulation of **$H_2$bcbpy·2Cl**, compounds **1** and **2** all exhibit obvious thermocontrolled fluorescence quenching phenomena. As displayed in Fig. S5,† when samples of **1** and **2** are heated at 90 °C for 5 min, they turn green. Therefore, as shown in Fig. 5, the emissions at 545 nm and 551 nm are absorbed by the colored samples, which results in quenching luminescence.

## The sensing of ammonia vapors

Recently, another type of Lewis acid site has been introduced into CPs based on bipyridinium (also called viologen) carboxylate linkers, which also have excellent electron-accepting abilities.[14–16] Because ammonia is a good electron donor and a Lewis base, the introduction of viologen moiety into coordination materials can impart selectivity for the visual sensing of amines. Along this line, compounds **1** and **2** were used to detect ammonia and are capable of sensing ammonia with high-contrast naked-eye color changes. Compound **1** and **2** turn to bottle-green and green, respectively, when exposed to ammonia vapor environment within 30 s (Fig. 6). After leaving **1** and **2** in air, **2** changes to light yellow again within 2 min, but **1** recovers to its original colour after 3 h in darkness. To explore the color change mechanism, the solid UV-vis diffuse reflectance spectra of **1** and **2** were measured. As shown in Fig. 4a, two new absorption bands with maxima at 621 nm and 748 nm appeared in the spectrum of **1-$NH_3$**. Such characteristic absorption bands

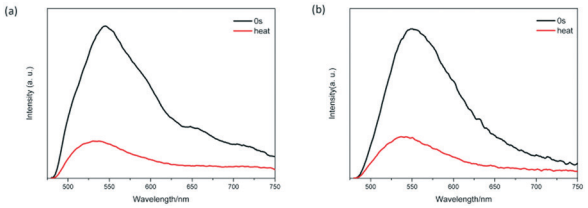


Fig. 5 The luminescence emission spectral changes ($\lambda_{ex}$ = 469 nm) of **1** (a) and **2** (b) after heating at 90 °C for 5 min.

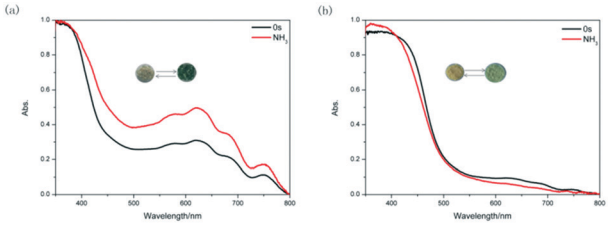


Fig. 6 (a) UV-vis spectra of compound **1** before and after the absorption of ammonia; (b) UV-vis spectra of compound **2** before and after the absorption of ammonia.

suggest that the ammonia-induced color change is likely to arise from the generation of the viologen free radicals. When compounds **1** and **2** were exposed to ammonia vapors, the ammonia molecules may act as electron donors to donate electrons to the bcbpy ligand to generate bcbpy free radicals. Compared with **1**, owing to the fast decoloration time, no new absorption bands appeared in the UV-vis spectrum of **2-$NH_3$** (Fig. 6b). The hugely different results for ammonia adsorption between **1** and **2** may mainly be due to the following two reasons: (1) as shown in Fig. 1, based on the packing structures of the two compounds, **1** has a similar 2D packing structure because of the helical 1-D structure, and such a structure facilitates ammonia absorption and storage; (2) except the Lewis acidic sites, unsaturated metal ions and bare carbonyl sites in **1** can provide the coordination possibility with ammonia molecules, especially the unsaturated metal ions sites, which usually make the materials unrecyclable owing to the structural collapse. As displayed in Fig. S11a,† the PXRD profiles show that the structure of **1** is collapsed. To further explore our conjecture, based on the X-ray crystallographic data of **1** and **2**, DFT calculations were performed to analyze the ammonia adsorption mechanism by

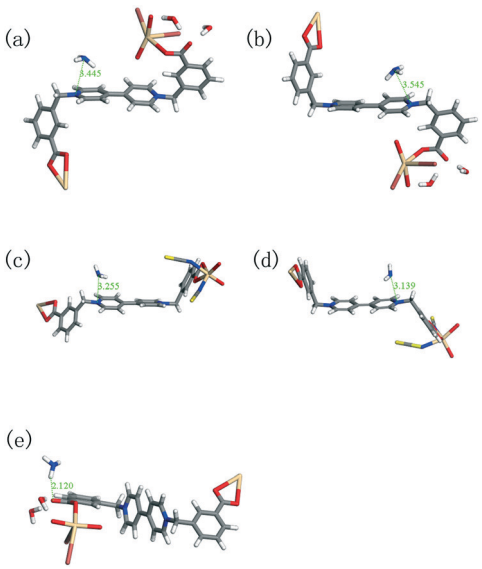


Fig. 7 The simulated ammonia adsorption mechanism progresses in **1** and **2**. (a) and (b) the interactions between the $N^+$ site of viologen and ammonia in **1**, (c) and (d) the interactions between the $N^+$ site of viologen and ammonia in **2** (e) the interactions between the carbonyl site and ammonia in **1**.

using MS 7.0. As displayed in Fig. 7, the simulated results suggest that the ammonia molecules as electron donors donate electrons to the bcbpy ligand to generate viologen free radicals. As expected, in compound **1**, a N–H···O hydrogen bond ($d$ = 2.120 Å) was formed between the ammonia molecule and the O atom of the carbonyl (Fig. 7e), which is another possible reason owing to the structural collapse for **1**. Comparing the difference ammonia detection results of the two complexes and other viologen-based CPs used for ammonia adsorption, it is worth noting that it is extremely rare that the carboxylate ligand-based CPs are stable upon ammonia adsorption. For instance MOF-74,[34] HKUST-1 (ref. 35) and other viologen–carboxylate CPs and MOFs[36,37] collapse during this step. In contrast, a recent work shows that a Cd-CP[16] based on viologen as **2**, whose metal center and carboxylate coordinate completely, remains stable upon ammonia adsorption.

## Conclusions

In summary, we have successfully prepared two novel multichromic Cd-CPs with a new flexible viologen ligand, which displayed rare reversible photochromism and thermochromism. Moreover, compounds **1** and **2** exhibit photo- and thermocontrolled luminescence properties in the solid state by ET. Interestingly, the two Cd-CPs can sense ammonia with high-contrast naked-eye color changes. Compound **2** remains stable upon ammonia adsorption. This systematic study illustrates the great potential applications of CPs based on viologens in photochemistry, thermochemistry and ammonia detection. This fact will motivate us to design and synthesize more multifunctional CPs based on viologens.

## Conflicts of interest

There are no conflicts to declare.

## Acknowledgements

We gratefully acknowledge the financial support from the NSF of China (21571032 21271038), the China High-Tech Development 863 program (2007AA03Z218) and the Analysis and Testing Foundation of Northeast Normal University.

## References

1 (*a*) A. G. Slater and A. I. Cooper, *Science*, 2015, **348**, 988; (*b*) X. Li, H. Xu, F. Kong and R. Wang, *Angew. Chem., Int. Ed.*, 2013, **52**, 13769; (*c*) A. Leblanc, M. Allain and N. Mercier, *Dalton Trans.*, 2017, **46**, 15666; (*d*) M. G. Campbell, S. F. Liu, T. M. Swager and M. Dincă, *J. Am. Chem. Soc.*, 2015, **137**, 13780.

2 M. Zhao, K. Yuan, Y. Wang, G. Li, J. Guo, L. Gu, W. Hu, H. Zhao and Z. Tang, *Nature*, 2016, **539**, 76.

3 (*a*) D. F. Weng, Z. M. Wang and S. Gao, *Chem. Soc. Rev.*, 2011, **40**, 3157; (*b*) X. Ma, D. Zhao, L. F. Lin, S. J. Qin, W. X. Zheng, Y. J. Qi, X. X. Li and S. T. Zheng, *Inorg. Chem.*, 2016, **55**, 11311; (*c*) M. Eddaoudi, J. Kim, N. Rosi, D. Vodak, J. Wachter, M. O'Keeffe and O. M. Yaghi, *Science*, 2002, **295**, 469.

4 (*a*) B. W. Qin, K. C. Huang, Y. Zhang, L. Zhou and J. P. Zhang, *Chem. – Eur. J.*, 2018, **24**, 1962; (*b*) Q. Yao, A. B. Goméz, J. Su, V. Pascanu, Y. Yun, H. Zheng, H. Chen, L. Liu, H. N. Abdelhamid, B. Martín-Matute and X. Zou, *Chem. Mater.*, 2015, **27**, 5332.

5 P. Falcaro, R. Ricco, C. M. Doherty, K. Liang, A. J. Hill and M. J. Styles, *Chem. Soc. Rev.*, 2014, **43**, 5513.

6 A. Dhakshinamoorthy and H. Garcia, *Chem. Soc. Rev.*, 2014, **43**, 5750.

7 P. Ramaswamy, N. E. Wong and G. K. H. Shimizu, *Chem. Soc. Rev.*, 2014, **43**, 5913.

8 Y. He, W. Zhou, G. Qian and B. Chen, *Chem. Soc. Rev.*, 2014, **43**, 5657–5678.

9 (*a*) R. Exelby and R. Grinter, *Chem. Rev.*, 1965, **65**, 247; (*b*) M. Irie, *Chem. Rev.*, 2000, **100**, 1685; (*c*) Y. Yokoyama, *Chem. Rev.*, 2000, **100**, 1717; (*d*) Y. Kishimoto and J. Abe, *J. Am. Chem. Soc.*, 2009, **131**, 4227; (*e*) L. Qin, L. P. Xu and L. Han, *Chem. Commun.*, 2013, **49**, 406.

10 (*a*) L. E. Kreno, K. Leong and J. T. Hupp, *Chem. Rev.*, 2012, **112**, 1105; (*b*) S. Shimomura and S. Kitagawa, *J. Mater. Chem.*, 2011, **21**, 5537.

11 L. Li, Y. Hua and H. Zhang, *Eur. J. Inorg. Chem.*, 2018, 3757–3760.

12 (*a*) D. C. Zhong, L. Q. Liao, J. H. Deng and X. Z. Luo, *Chem. Commun.*, 2014, **50**, 15807; (*b*) J. Z. Liao, C. Wu, X. Y. Wu and C. Z. Lu, *Chem. Commun.*, 2016, **52**, 7394.

13 (*a*) J. Park, D. Feng, S. Yuan and H. C. Zhou, *Angew. Chem., Int. Ed.*, 2015, **54**, 430; (*b*) J. Park, Q. Jiang, D. Feng and H. C. Zhou, *Angew. Chem., Int. Ed.*, 2016, **55**, 7188.

14 H. Y. Li, Y. L. Wei and S. Q. Zang, *Chem. Mater.*, 2015, **27**, 1327.

15 H. Y. Li, H. Xu and S. Q. Zang, *Chem. Commun.*, 2016, **52**, 525.

16 Q. Sui, P. Li, N. N. Yang and E. Q. Gao, *ACS Appl. Mater. Interfaces*, 2018, **10**, 11056.

17 X. Y. Chen, N. N. Zhang, L. Z. Cai, P. X. Li, M. S. Wang and G. C. Guo, *Chem. – Eur. J.*, 2017, **23**, 7414.

18 Q. X. Yao, Z. F. Ju, X. H. Jin and J. Zhang, *Inorg. Chem.*, 2009, **48**, 1266.

19 Y. Z. Zhang, D. F. Li, R. Clérac, M. Kalisz, C. Mathonire and S. M. Holmes, *Angew. Chem., Int. Ed.*, 2010, **49**, 3752.

20 Y. N. Gong and T. B. Lu, *Chem. Commun.*, 2013, **49**, 7711.

21 (*a*) Q.-L. Zhu, T.-L. Sheng and X.-T. Wu, *Chem. – Eur. J.*, 2011, **17**, 3358; (*b*) Z.-Y. Fu, Y. Chen, J. Zhang and S.-J. Liao, *J. Mater. Chem.*, 2011, **21**, 7895.

22 P. X. Li, M. S. Wang and G. C. Guo, *J. Mater. Chem. C*, 2015, **3**, 253.

23 O. V. Dolomanov, L. J. Bourhis, R. J. Gildea, J. A. K. Howard and H. Puschmann, *J. Appl. Crystallogr.*, 2009, **42**, 339.

24 G. Sheldrick, *Acta Crystallogr., Sect. A: Found. Crystallogr.*, 2008, **64**, 112.

25 (*a*) B. Delley, *J. Chem. Phys.*, 2000, **113**, 7756–7764; (*b*) B. Delley, *J. Chem. Phys.*, 1990, **92**, 508.

 

26 *Materials Studio. version 5.0.0*, Accelrys Software Inc., SanDiego, CA, 2009.
27 J. P. Perdew, K. Burke and M. Ernzerhof, *Phys. Rev. Lett.*, 1996, **77**, 3865.
28 A. Tkatchenko and M. Scheffler, *Phys. Rev. Lett.*, 2009, **102**, 3005.
29 C. Chen, J.-K. Sun, Y.-J. Zhang, X.-D. Yang and J. Zhang, *Angew. Chem., Int. Ed.*, 2017, **56**, 14458.
30 J. Z. Liao, H. L. Zhang, S. S. Wang, J. P. Yong, X. Y. Wu, R. Yu and C.-Z. Lu, *Inorg. Chem.*, 2015, **54**, 4345.
31 J. Liu, P. X. Li, H. Y. Zeng and G. C. Guo, *RSC Adv.*, 2017, **7**, 34901.
32 Q. Sui, X. T. Ren, Y. X. Dai, E. Q. Gao and L. Wang, *Chem. Sci.*, 2017, **8**, 2758.
33 C. X. Ren, A. L. Zheng, L. X. Cai and J. Zhang, *CrystEngComm*, 2014, **16**, 1038.
34 M. J. Katz, A. J. Howarth, P. Z. Moghadam and O. K. Farha, *Dalton Trans.*, 2016, **45**, 4150.
35 C. Petit, L. Huang, J. Jagiello, J. Kenvin, K. E. Gubbins and T. J. Bandosz, *Langmuir*, 2011, **27**, 13043.
36 M. Leroux, N. Mercier, M. Allain, M.-C. Dul, J. Dittmer and I. Bezverkhyy, *Inorg. Chem.*, 2016, **55**, 8587.
37 M. Leroux, N. Mercier, J. Bellat, G. Weber and I. Bezverkhyy, *Cryst. Growth Des.*, 2017, **17**, 2828.